Nigerian Journal of Solar Energy, Vol. 28, 2017.

Performance Evaluation and Modelling of Amorphous Silicon Photovoltaic Module in Minna, Nigeria

[1]Ezenwora, J. A., [2]Oyedum, O. D., [3]Ugwuoke, P. E. and [4]Olomiyesan, B. M.
[1, 2]Department of Physics, Federal University of Technology, Minna, Nigeria.
[3]National Centre for Energy Research and Development, University of Nigeria, Nsukka.
[4]Examination Development Department, National Examinations Council (NECO).

Abstract *- The performance response of amorphous silicon Photovoltaic (PV) module to ambient parameters of solar irradiance, temperature, wind speed and relative humidity, was investigated in Minna (Nigeria) local environment, using Campbell Scientific CR1000 software-based data acquisition system. The PV modules under test and meteorological sensors were installed on a metal support structure at the same test plane. The data monitoring was from 8.00 am to 6.00 pm (sunrise to sunset) each day continuously for a period of one year, from December 2014 to November 2015. Maximum value of module efficiency of 3.61% for the amorphous module was recorded at irradiance of 536.5 W/m^2. At 1000 W/m^2 the efficiency reduced to 2.25 %, as against manufacturer's specification of 33 % for the module. The maximum power output achieved for the module at irradiance of 1000 W/m^2 was 0.652 W representing 6.52 % of the manufacturer's power specification for the module. Accordingly, Module Performance Ratio (MPR) for the PV module is 0.07. The rate of variation of module response variables with irradiance and temperature was determined using a linear statistical model given as* $Y = a + bHg + cTmod$. *The coefficient of determination for the fits for the performance variables are: 65.3 %, 92.1 %, 65.0 % and 65.0 % for the open-circuit voltage, short-circuit current, power and maximum power respectively. The overall lack of fit tests for these performance variables is significant at probability, P value of 0.000, signifying good fits.*

Keywords - Module, Photovoltaic, Amorphous, Ambient, Statistical

1.0 INTRODUCTION

The need to characterise and evaluate the performance of photovoltaic modules in order to ensure optimal performance and technical quality in photovoltaic power systems has often been pointed out (Almonacid *et al.*, 2009). The effect of deviation of meteorological parameters from Standard Test Condition (STC), together with the fact that PV modules with actual power smaller than the nominal value can still be found in the market lend credence to this. Essentially, PV power system design involves electrically-matching power components and ultimately, the power supply to the load. STC are easily recreated in a factory, and allow for consistent comparisons of products, but need to be modified to estimate output under common outdoor operating conditions. Module output power reduces as module temperature increases. The rate of decrease of output power with temperature for a particular locality ought to be understood and the loss factor for each module type in every location established. These loss factors need to be documented and applied in order to effectively estimate system output and sizing before installation. This will lead to the design and installation of efficient PV power system that is reliable, dependable and durable. In developed world such as the United States of America (USA) which is a lead actor in PV research, there have been efforts to conduct outdoor tests of modules and array performance since 1976 through the Sandia National Laboratory. The US has effectively established and documented loss factors for all losses affecting PV power systems for all PV module types and for every location (California Energy Commission, 2001).

Realistic outdoor performance analysis of various types of modules is needed in developing countries such as Nigeria, in order to be able to effectively design and size arrays for different applications and sites. It is no longer news that Nigeria is an energy resource rich country, blessed with both fossil fuel reserves such as crude oil, natural gas, coal, and renewable energy resources like solar, wind, biomass, biogas and hydropower resources. It is also true that despite the abundance of these energy resources in Nigeria, the country is in short supply of electrical power. There is supply-demand gap particularly in view of the growing energy demand in the domestic, commercial and industrial sectors of the economy, and the reason for this is not farfetched. The National energy supply is at present almost entirely dependent on fossil

*Corresponding author Tel: +234-8053331748
Email: aghaegbunam@yahoo.com

fuels, firewood (which are depleting fast) and hydropower. The capacity utilisation of hydropower plants over the recent years has been low at about 30% only (Umar, 1999). According to Umar (1999), Grid power generation capacity in Nigeria as at 1990s was about 1,800 MW or 31% of the installed capacity and according to Okafor and Joe-Uzuegbu (2010), less than 40% of the 150 million Nigerians in the country are supplied electricity from the national grid in the urban centres while in the rural centres, where about 70% of the population live, the availability of electricity drops to 15%. Nigeria with an annual population growth rate of about 2.8% (according to 2006 population census), the total Electricity generation capacity as at 2010 stood at less than 4000 MW with per capita consumption of 0.03 kW. With these figures, the level of shortage in Electricity supply becomes evident, resulting in consistent unreliability and epileptic nature of electricity supply in the country.

While the initial capital investment may be higher, PV power system provides electrical power at less cost than electricity from generator, based on life-cycle cost. Because it has an added advantage of requiring little maintenance, low running costs and being environmentally friendly. PV power is the most reliable source of electricity ever invented and it is portable, easily installed, and virtually maintenance-free (Midwest Renewable Energy Association Fact Sheet , 2013). Therefore, this study was carried out to determine the realistic outdoor performance of amorphous silicon PV module in Minna environment for effective design and sizing of PV power system.

2.0 METHODOLOGY

2.1 Monitoring Stage

The performance response of amorphous silicon PV module to ambient weather parameters; solar irradiance, temperature, wind speed and relative humidity, was monitored in Minna environment, using CR1000 software-based data logging system with computer interface. The PV module under test, and meteorological sensors, were installed on support structure at the same test plane, at about three metres of height, so as to ensure adequate exposure to insolation and enough wind speed, since wind speed is proportional to height. The elevation equally ensures that the system is free from any shading from shrubs and also protected from damage or interference by intruders. Also, the whole experimental set up was secured in an area of about four metres in diameter. The modules were tilted at approximately 10º (since Minna is on latitude 09º37' N) to horizontal and south-facing to ensure maximum insolation (Strong and Scheller, 1991; Ugwuoke *et al.*, 2005). The data monitoring was from 8.00am to 6.00pm local time, each day continuously for a period of one year, spanning from December 2014 to November 2015, so as to cover the two distinct and well defined climate seasons of the area. The experiment was carried out near Physics Department, Federal University of Technology, Minna (latitude 09º37' N, longitude 06º32' E and 249 metres above sea level). The sensors were connected directly to the CR1000 Campbell Scientific data logger, while the module was connected to the logger via electronic load specifically designed for the module. The logger was programmed to scan the load current from 0 to 1 A at intervals of 50 mA every 5 minutes, and average values of short-circuit current, I_{sc}, open-circuit voltage, V_{oc}, current at maximum power, I_{max}, voltage at maximum power, V_{max}, power and maximum power obtained from the module together with the ambient parameters are recorded and logged. Data download at the data acquisition site was performed every 7 days to ensure effective and close monitoring of the data acquisition system (DAS). At the end of each month and where necessary, hourly, daily and monthly averages of each of the parameters - solar (global) irradiance, solar insolation, wind speed, ambient and module temperatures, and the output response variables (open-circuit voltage, V_{OC}, short-circuit current, I_{SC}, voltage at maximum power, V_{max} , current at maximum power, I_{max}, efficiency, Eff and fill factor, FF) of the photovoltaic module was obtained. The global solar radiation was monitored using Li-200SA M200 Pyranometer, manufactured by LI-COR Inc. USA, with calibration of 94.62 microamperes per 1000 W/m^2. The ambient temperature and relative humidity were monitored using HC2S3-L Rotronic HygroClip2 Temperature/Relative Humidity probe, manufactured in Switzerland. Wind speed was monitored using 03002-L RM Young Wind Sentry Set. And module temperature was monitored using 110PV-L Surface-Mount Temperature probe. All sensors are installed in the CR1000 Campbell Scientific data logger with measurement and control module. Table 1 shows the manufacturer’s specifications at STC of the module investigated while Plate I shows the data acquisition set up.

Table 1: Manufacturer's Specifications at STC and Measured Dimensions of the Solar Module

Cell Technology	No of Cells per Module	Max. Rated Power (W)	Max. Rated Voltage (V)	Max. Rated Current (A)	Open-Circuit Voltage (V)	Short-Circuit Current (A)	Module Dimensions (m x m)	Cell Dimensions (m x m)	Total Surface Area of Cells	Model/ Make	Eff (%)
Amorphous Module	17 Cells in single series	10	17.4	0.55	21.2	0.62	0.30 x 0.12	0.1 x 0.017	0.0289	SLP 10-12 /China	33*

*Module efficiency was calculated because it was not included in the manufacturer's specifications

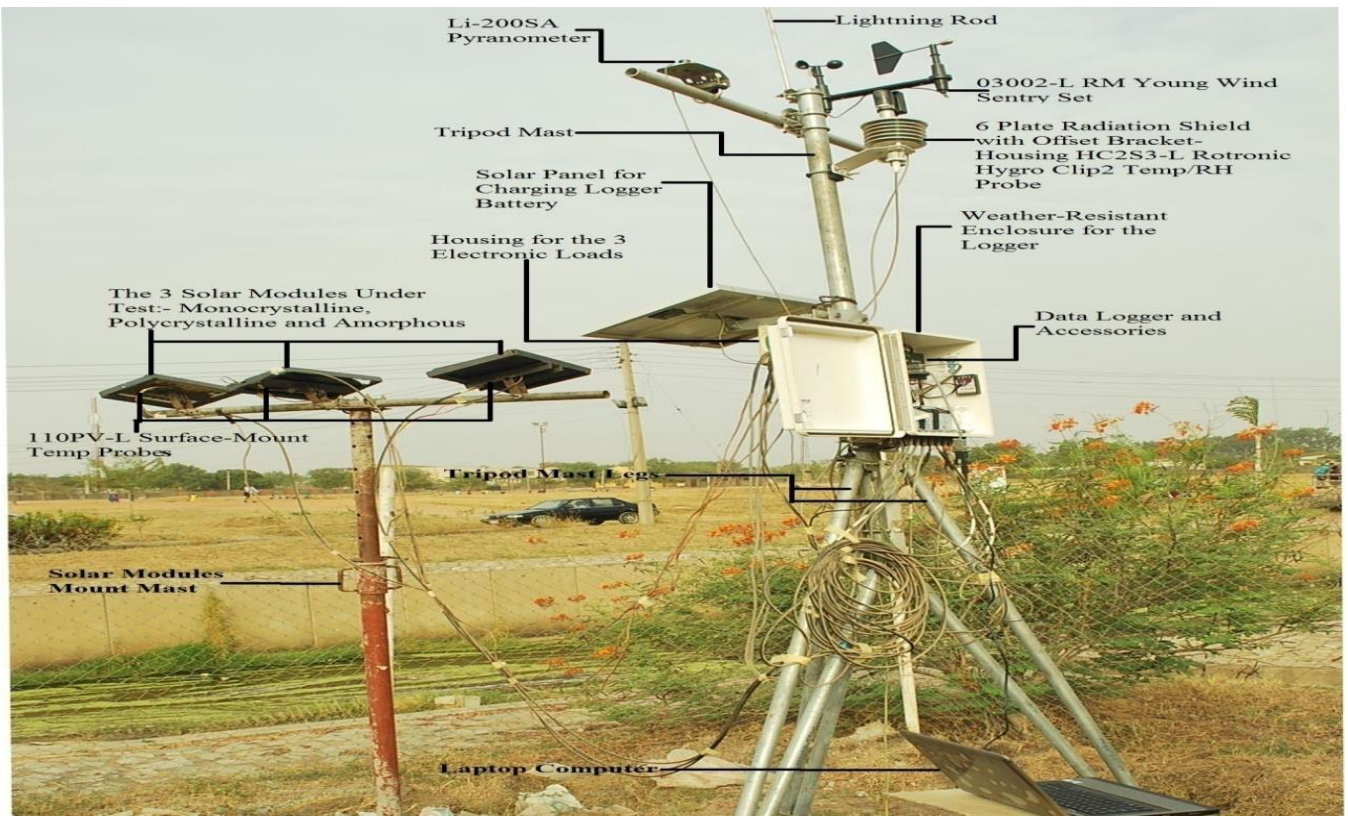

Plate I: The Experimental Set up

2.2 Data Analysis

Performance response of the module to ambient weather parameters was investigated in terms of open-circuit voltage, V_{OC}, short-circuit current, I_{SC}, voltage at maximum power, V_{max} , current at maximum power, I_{max} , efficiency, Eff and fill factor, FF. Fill Factor, FF, Efficiency, Eff, and Module Performance Ratio (MPR) were evaluated using the following expressions:

Fill Factor, FF = $I_{max}\,V_{max}/I_{sc}V_{oc}$ (1)

Efficiency,Eff= $I_{max}\,V_{max}/P_{in}$=$I_{sc}V_{oc}\ FF/P_{in}$=$I_{sc}V_{oc}\ FF/AE_e$ (2)

$Module\ Performance\ Ratio\ (MPR) = Effective\ Efficiency/Efficiency\ at\ STC$ (3)

In order to further determine the rate of variation of module response variables with meteorological parameters, especially irradiance and temperature, statistical analysis was performed on the observed data with the aid of statistical package; Minitab 17 and linear statistical models for prediction of performance variables are presented. Multiple regression models, analysis of variance (ANOVA) and correlation between the variables were considered with the aim of establishing the statistical significant relationship between the variables and the goodness of fit of the models for the research study. The regression equation is;$Y = a + bHg + c\,Tmod$ (4)

where Y is the output response parameter being predicted, H_g is global radiation (solar irradiance) and T_{mod} is module temperature. The coefficients b and c are the rates of variation of output variables with respect to irradiance and module temperature, respectively while a is intercept on the Y axis.

The I-V curves were produced by plotting current against voltage produced by the logger in scanning the electronic load current from 0 to 1 A at intervals of 50 mA. The maximum power point, P_{max}, which is the operating point of the module, was equally recorded by the logger.

3.0 RESULTS AND DISCUSSION

Figure 1 shows the output characteristics of the amorphous silicon PV module as functions of global irradiance. This output characteristics is expressed in the form of I-V curves.

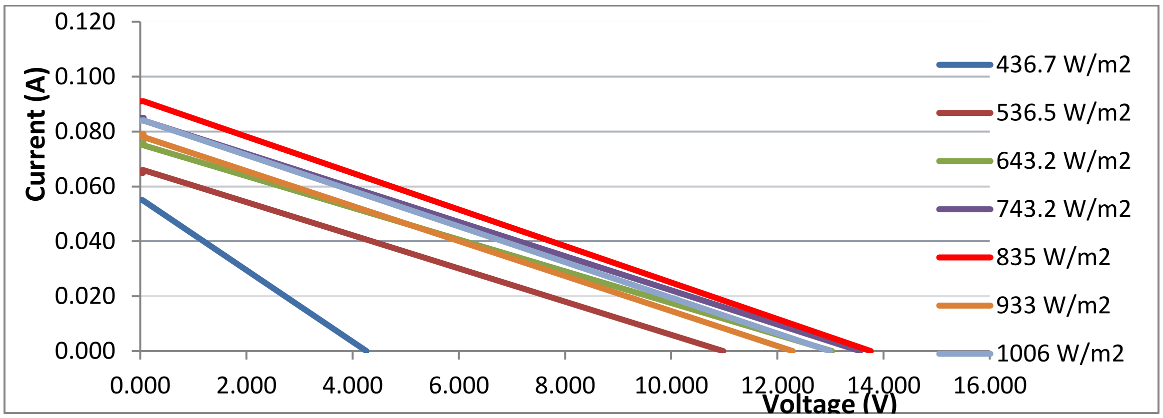

Figure 1: I-V Characteristics for the amorphous silicon module as a function of global irradiance

This I-V characteristics is worthy of note because it does not depict diode characteristics that is usually associated with solar modules. This is because the manufacturer's specifications are particularly too unrealistic that its effective performance is far below the range of the electronic load designed for it based on the specifications of the manufacturer. Although its current at maximum power, I_{max}, according to the manufacturer's specification is 0.55 amperes, it could not deliver 0.05 amperes of current at the first step of the load current (50 mA). This explains the sudden descent in the characteristic curve immediately it was loaded, giving slanting lines instead of curves as seen in Figure 1. The open-circuit voltage, V_{oc}, is seen to increase with increase irradiance up to 835 W/m^2 after which it witnessed a decrease. This is due to high temperature associated with high irradiance value that has adverse effect on open-circuit voltage. On the contrast, the increase in short-circuit current with irradiance is more linear as seen in the regular spacing on the current axis. This contrast in open-circuit voltage and short-circuit current is more glaring in Figures 2 and 3 where these performance variables are compared with module temperature at various irradiance levels.

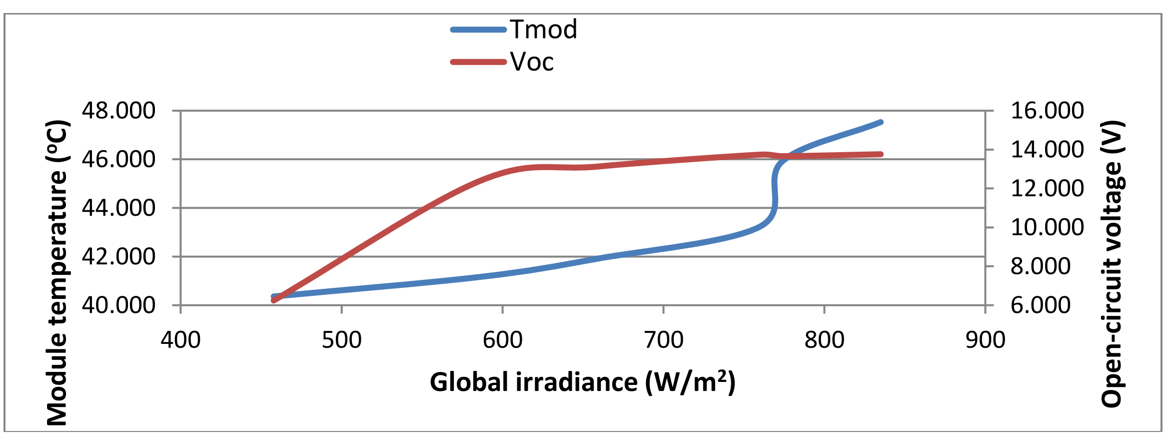

Figure 2: Variation of open-circuit voltage and module temperature as a function of global irradiance

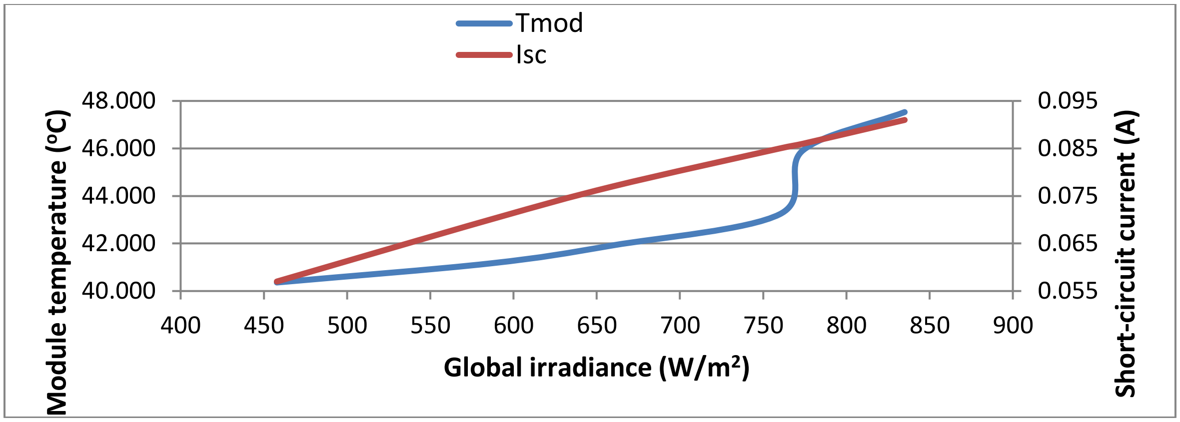

Figure3: Variation of short-circuit current and module temperature as a function of global irradiance

It is obvious then that the open-circuit voltage does not have linear relationship with module temperature and hence solar irradiance as against short-circuit current that increased steadily. This result is in agreement with Ugwuoke and Okeke (2012).

The relationship of maximum power point and efficiency to temperature variations was investigated and shown in Figures 4 and 5 respectively.

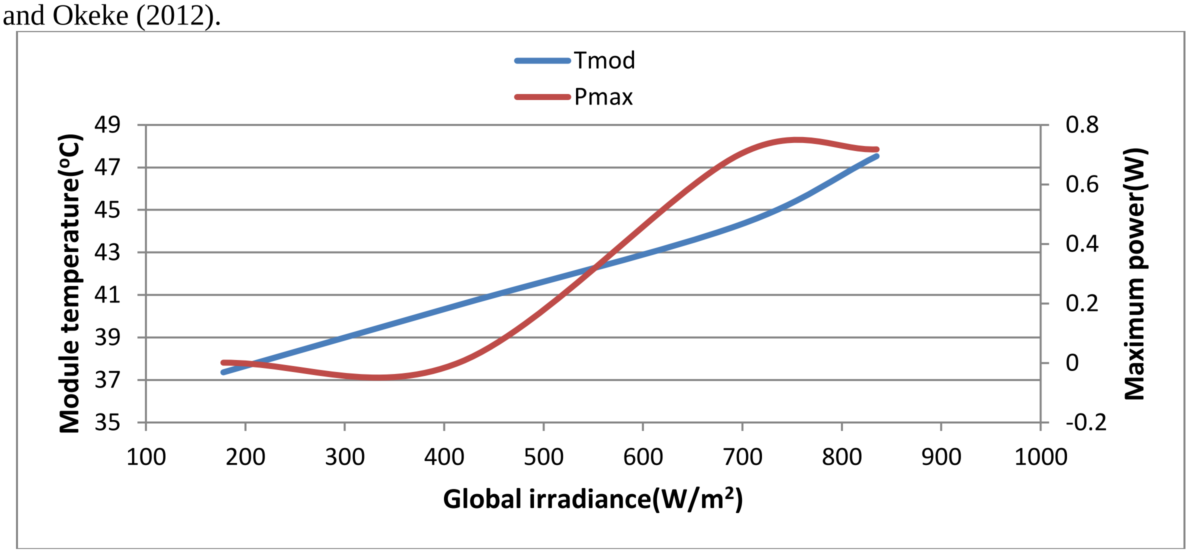

Figure 4: Variation of Maximum Power Point (MPP) and module temperature at different levels of irradiance

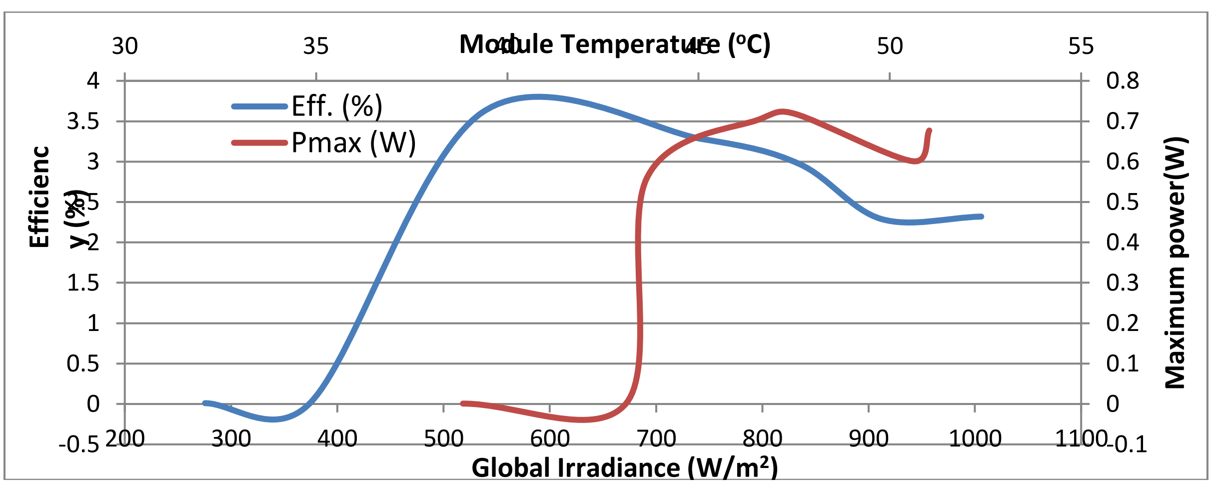

Figure 5: Variation of efficiency and maximum power point as a function of global irradiance and module temperature

As shown in these Figures the maximum power point increases with increase in solar irradiance of about 800 W/m^2. This explains the inclusion of Maximum Power Point Tracker (MPPT) in some photovoltaic power system components. Maximum power point and efficiency show symmetrical structure at irradiance of about 600 W/m^2 to 700 W/m^2. This is in agreement with some earlier works (Bajpai and Gupta, 1986; Ugwuoke, 2005). Monthly hourly averages of open-circuit voltage, short-circuit current, power output and maximum power are investigated and the plots for a typical dry season month (January) and a typical rainy season month (August) are shown in Figures 6 to 9.

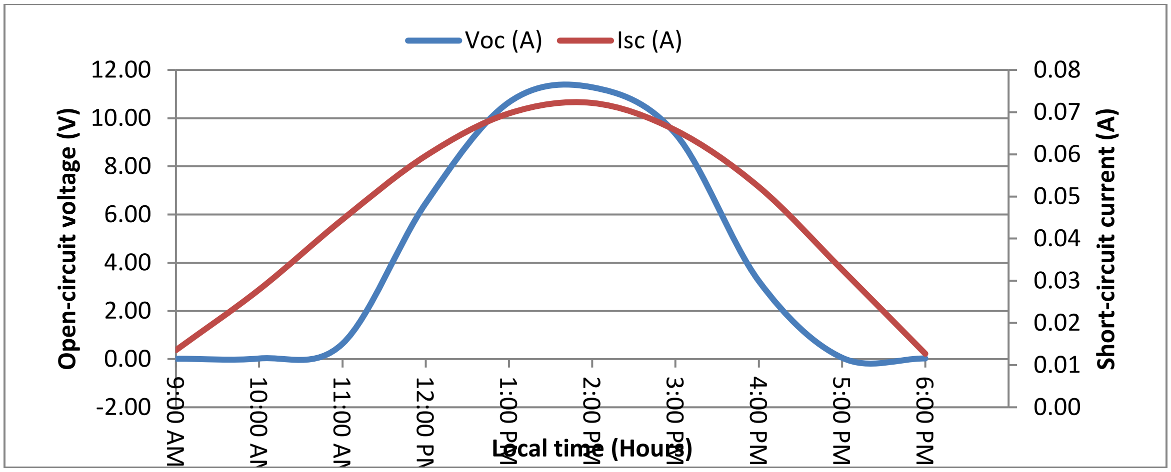

Figure 6: Hourly average variation of open-circuit voltage and short-circuit current as a function of time for the month of January 2015

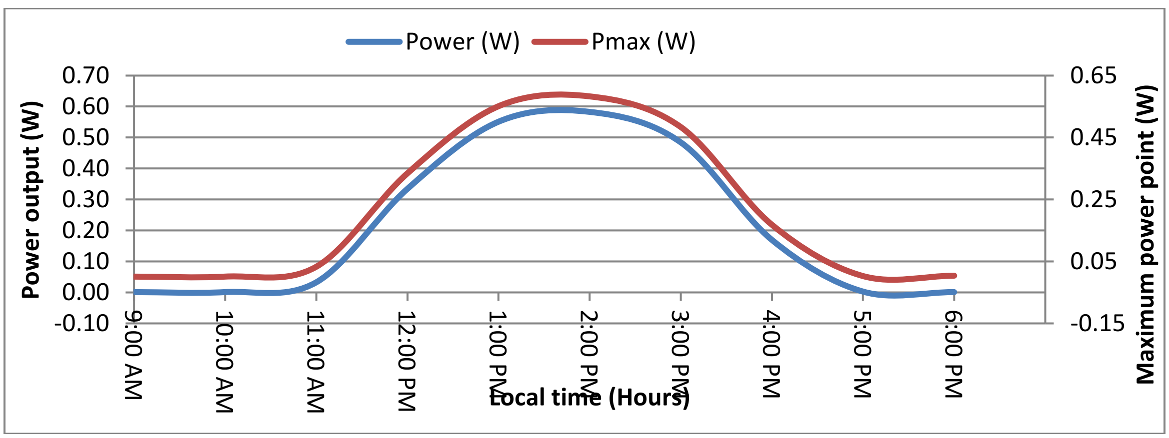

Figure 7: Hourly average variation of power and maximum power as a function of time for the month of January 2015

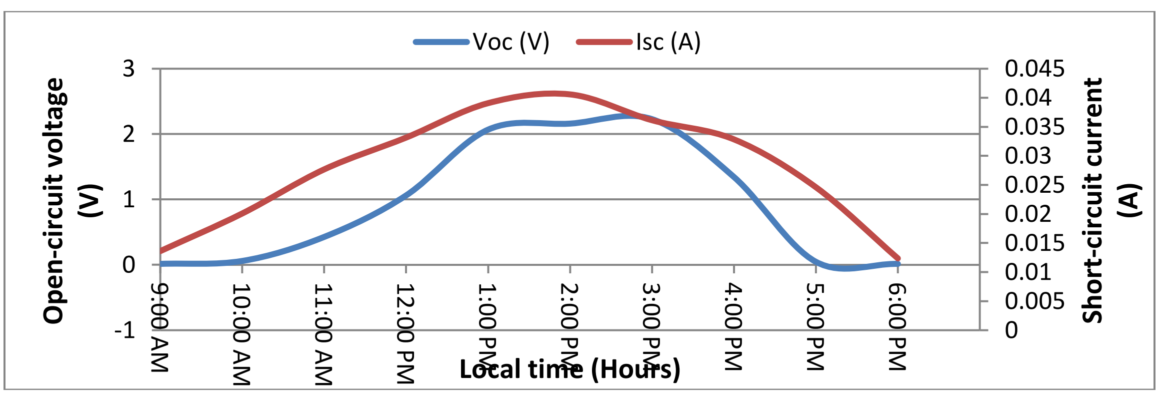

Figure 8: Hourly average variation of open-circuit voltage and short-circuit current as a function of time for the month of August 2015

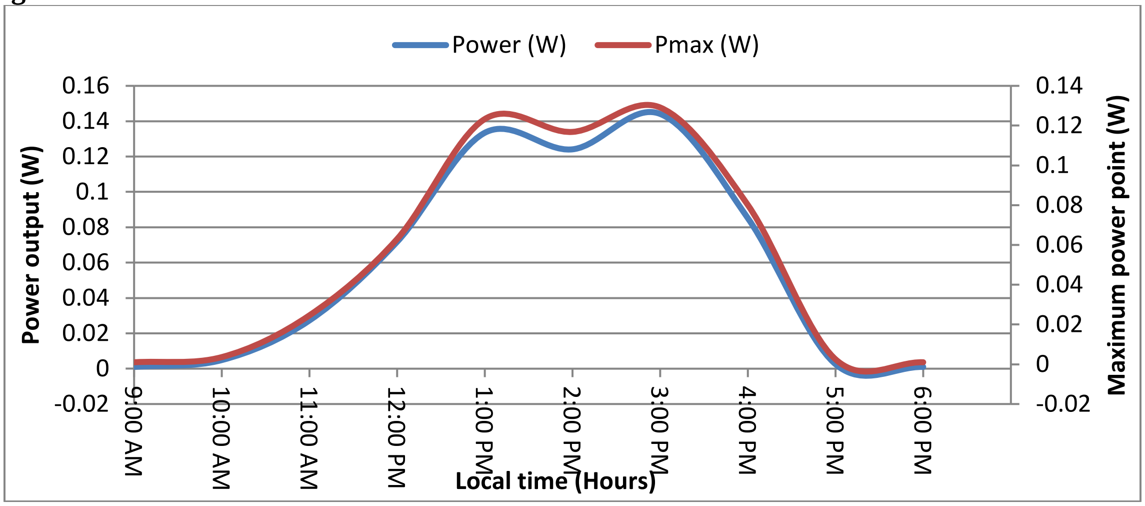

Figure 9: Hourly average variation of power and maximum power as a function of time for the month of August 2015

The peak time for the performance variables of the module is in the afternoon for the two climatic seasons, at 2:00 pm and 3:00 pm local time, which is the peak time of module temperature, confirming that amorphous silicon module performance variables are less affected by high temperature. Its power output curves overlap with the maximum power curves, their scales are slightly made different in order for the two curves to be visible.

Hourly average values of the module performance variables and ambient parameters for the one year duration of this study are shown in Table 2.

Table 2: Annual hourly averages of ambient parameters and performance variables

T (Hours)	H_g (W/m^2)	T_a (°C)	T_{mod} (°C)	V_{oc} (V)	I_{sc} (A)	Power (W)	P_{max} (W)	RH (%)	WS (m/s)
9:00 AM	258	26.5	27.4	0.02	0.017	0.001	0.001	65.3	1.99
10:00 AM	427	27.8	30.3	0.42	0.030	0.023	0.023	61.8	2.18
11:00 AM	569	29.1	32.9	2.11	0.043	0.113	0.112	54.5	2.17
12:00 PM	666	30.3	35.4	5.02	0.054	0.264	0.262	53.2	2.08
1:00 PM	708	31.3	37.3	6.99	0.060	0.366	0.364	51.5	2.02
2:00 PM	696	32.2	38.5	7.29	0.061	0.382	0.379	48.8	1.93
3:00 PM	608	32.7	38.6	5.89	0.054	0.316	0.313	47.3	1.87
4:00 PM	482	33.0	38.0	1.99	0.044	0.112	0.109	45.7	1.82
5:00 PM	309	32.9	36.4	0.06	0.028	0.003	0.003	44.9	1.71
6:00 PM	139	31.9	33.2	0.02	0.013	0.001	0.002	46.2	1.59

The monthly average values of solar irradiance, wind speed and relative humidity together with open-circuit voltage, short-circuit current, maximum power and module temperature for the amorphous module is presented in Table 3. It was observed here that wind speed peaked in the month of January, during the dry season of the study area, normally characterised by strong North-East trade wind and favours open-circuit voltage more than short-circuit current (amidst other factors). Also it is observed that module temperature recorded relatively low value, vis-a-vis their irradiance levels during this month. This is because high wind speed leads to increased rate of heat transfer from the module to the ambient resulting in the low module temperature.

Table 3: Monthly average values of ambient parameters and performance variables

Month	H_g (W/m^2)	WS (m/s)	RH (%)	V_{oc} (V)	I_{sc} (A)	P_{max} (W)	T_{mod} (°C)
Dec 14	509.5	1.68	32.08	4.707	0.046	0.243	36.26
Jan 15	529.8	1.99	25.97	4.146	0.045	0.214	34.41
Feb 15	529.6	1.59	32.06	3.447	0.043	0.178	37.95
Mar 15	537.6	1.88	33.14	2.664	0.040	0.138	38.18
Apr 15	569.0	1.70	31.99	2.201	0.040	0.114	39.52
May 15	509.9	1.81	55.87	2.408	0.040	0.124	36.33
Jun 15	424.3	1.74	71.40	1.447	0.032	0.075	32.10
Jul 15	415.7	1.68	73.14	1.587	0.032	0.082	31.45
Aug 15	326.4	1.45	81.08	0.944	0.028	0.049	29.32
Sep 15	415.8	1.47	74.15	2.195	0.037	0.113	31.60
Oct 15	479.9	1.39	70.18	3.697	0.046	0.191	33.88
Nov 15	557.9	1.41	35.34	6.085	0.055	0.314	36.98

Relative humidity peaked in the month of August, which is the peak of rainy season of the study area and leads to lowest insolation level also witnessed in this month because increased water content in the atmosphere gives rise to cloudy weather which results in the absorption and scattering of sun's rays. Other factors being equal, high relative humidity brings about low module temperature which would normally favour open-circuit voltage more than short-circuit current, but with such very high value of relative humidity as recorded in August, its effect becomes domineering and results in very low insolation level that dictates the results of other parameters as is shown in the Table, and that explains the lowest recorded values of all the performance variables for the module.

The performance of the amorphous photovoltaic module at different levels of solar irradiance (global irradiance) for the period studied were summarised in Table 4. Fill factor and efficiency at the different levels of irradiance for the module were also computed and inserted.

Table 4: Summary of performance response for the module at different irradiance levels

Irradiance (W/m^2)	V_{oc} (V)	I_{sc} (A)	P_{max} (W)	V_{max} (V)	I_{max} (A)	FF	Eff (%)
276	0.03	0.035	0.001	0.025	0.036	1.029	0.01
375	0.04	0.047	0.002	0.035	0.048	0.894	0.02
437	4.26	0.055	0.222	4.261	0.052	0.946	1.76
537	10.98	0.065	0.558	10.980	0.051	0.785	3.61
643	13.03	0.075	0.670	13.030	0.051	0.680	3.58
743	13.56	0.085	0.707	13.560	0.052	0.612	3.28
835	13.76	0.091	0.718	13.760	0.052	0.571	2.97
912	11.83	0.077	0.601	11.830	0.051	0.662	2.29
933	12.29	0.079	0.641	12.290	0.052	0.658	2.37

1000	12.50	0.080	0.652	12.500	0.052	0.650	2.25

T_{mod} = 37.7^{o}C,
MPR = 0.07
Pmax (%) = 6.52%

For comparison between the outdoor module performance and the Standard Test Condition (STC) specifications, module performance ratio (MPR), module temperature and maximum power at 1000 W/m^2 are equally presented. The maximum power output achieved for the module at 1000 W/m^2 was 0.652 W representing 6.52 % of the manufacturer's power specifications for the amorphous photovoltaic module. Module efficiency is seen to decrease steadily as solar irradiance increased with maximum value of 3.61 % at irradiance of 536.5 W/m^2. This maximum value then decreased steadily with increased irradiance and at 1000 W/m^2 the efficiency reduced to 2.25 % as against manufacturer's specification of 33 %. Open-circuit voltage at 1000 W/m^2 was 12.5 V as against manufacturer's specification of 21.2 V, while the short-circuit current was 0.080 A as against manufacturer's specification of 0.62 A. Maximum current, I_{max} recorded 0.052 A, as against STC value of 0.55 A. Therefore, module performance ratio for the PV module under investigation is 0.07 and it was equally observed here that the module did not record module temperature of 25 ^{o}C at 1000 W/m^2 solar irradiance as usually assumed for STC condition, rather, as seen in Table 4, the module temperature is well beyond 25 ^{o}C in the local environment. It is then quite clear and obvious, given the enormous margin of deviation of the outdoor characterised values from the manufacturer's STC specifications, that STC data is suspect; it is only handy in making comparison among solar modules. Designing with manufacturer's STC data will produce an unreliable and defective PV power system. In addition, over specified modules are flooding our local market.

3.1 Results of Statistical Analysis and Models

Models for V_{oc}, I_{sc}, P and P_{max} were analysed in this section.
The regression equation for V_{oc} is $Voc = -6.46 + 0.0109\,Hg + 0.110\,Tmod$ (5)
where H_g is solar (global) irradiance and T_{mod} is module temperature

Table 5: Predictor coefficient for the independent variables and the T-test value for equation 5

Predictor	Coefficient	SE Coefficient	T-test	P-value	VIF
Constant	-6.458	1.414	-4.57	0.000	
H_g	0.010913	0.001211	9.01	0.000	1.6
T_{mod}	0.11006	0.04859	2.27	0.026	1.6

From Table 5 the coefficient of H_g and T_{mod} are statistically significant since the P-value = 0.000 and 0.026 respectively are less than 0.05 (5%) level of significance. And from equation 5, V_{oc} – axis has an intercept of -6.46, and for every unit increase in H_g there is an increase of 0.0109; also for every unit increase in T_{mod}, there is a positive increase of 0.110 in the model.

Table 6: Regression Analysis of variance (ANOVA) of the model for equation 5

Source	Degree of freedom	Sum of squares	Mean square	F-test	P-value
Regression	2	692.53	346.26	91.17	0.000
Residual Error	97	368.40	3.80		
Total	99	1060.93			

S = 1.94884 R-Sq = 65.3% R-Sq (adj) = 64.6%

From Table 6, since the P-value = 0.000 is less than 5% (0.05) level of significance; it can be concluded that there is statistically significant difference in the contributions of the variables H_g and T_{mod} in the model. This is further explained by the coefficient of determination R^2 = 65.3% that is 65.3% of the variable was explained by the model, while only 34.7% was unexplained. The model in equation 5 is a good model.
Overall lack of fit test is significant at P = 0.000.
From Table 7, the coefficient of Hg and Tmod are statistically significant since the P-value = 0.000 is less than 0.05 (5%) level of significance. From equation 6, Isc

– axis has an intercept of -0.0159, and for every unit increase in Hg there is an increase of 0.000072, also for every unit increase in Tmod, there is a positive increase of 0.000577 in the model.

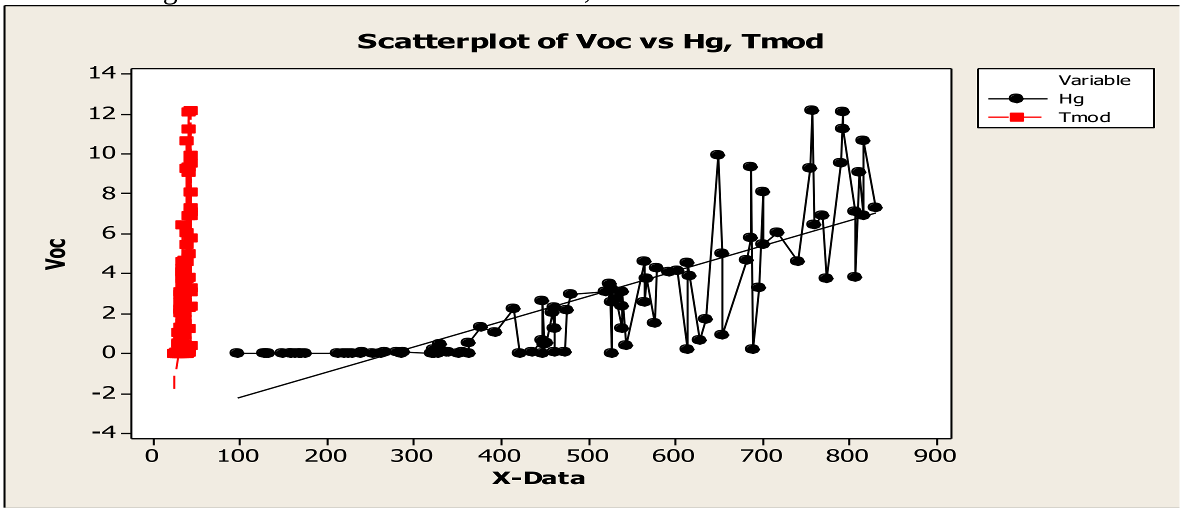

Figure 10: Scatter plot of V_{oc} versus H_g and T_{mod} for the amorphous module

The regression equation for I_{sc} is $Isc = -0.0159 + 0.000072\,Hg + 0.000577\,Tmod$ (6)

Table 7: Predictor coefficient for the independent variables and the T-test value for equation 6

Predictor	Coefficient	SE Coefficient	T-test	P-value	VIF
Constant	-0.015892	0.0003612	-4.40	0.000	
H_g	0.00007156	0.000000309	23.13	0.000	1.6
T_{mod}	0.0005771	0.0001242	4.65	0.000	1.6

Table 8: Regression Analysis of variance (ANOVA) of the model for equation 6

Source	Degree of freedom	Sum of Square	Mean Square	F-test	P-value
Regression	2	0.027933	0.013966	563.22	0.000
Residual Error	97	0.002405	0.000025		
Total	99	0.030338			
S = 0.00497966	R-Sq = 92.1%	R-Sq (adj) = 91.9%			

From Table 8, since the P-value = 0.000 is less than 5% (0.05) level of significance; it can be concluded that there is statistically significant difference in the contributions of the variables H_g and T_{mod} in the model. This is further explained by the coefficient of determination R^2= 92.1% that is 92.1% of the variable was explained by the model, while only 7.9 % was unexplained. The model in equation 6 is a good model and no evidence of lack of fit since P = 0.000. From Table 9 the coefficient of H_g and T_{mod} are statistically significant since the P-value = 0.000 is less than 0.05(5%) level of significance. From equation 7, P – axis has an intercept of -0.316, and for every unit increase in Hg there is an increase of 0.000574, also for every unit increase in T_{mod}, there is a positive increase of 0.00515 in the model. From Table 10, since the P-value = 0.000 is less than 5% (0.05) level of significance; it can be concluded that there is statistical significant difference in the contributions of the variables H_g and T_{mod} in the model. This is further explained by the coefficient of determination R^2= 65.0% that is 65.0% of the variable was explained by the model, while only 35.0% was unexplained. The model in equation 7 is a good model. Overall lack of fit test is significant at P = 0.000. From Table 11, the coefficient of Hg and Tmod are statistically significant since the P-value = 0.000 and is less than 0.05 (5%) level of significance. Form equation 8, Pmax – axis has an intercept of -0.324, and for every unit increase in Hg there is an increase of 0.000567, also for every unit increase in Tmod, there is a positive increase of 0.00542 in the model. The regression equation for P is

$P = -0.316 + 0.000578\,Hg + 0.00515\,Tmod$ (7).

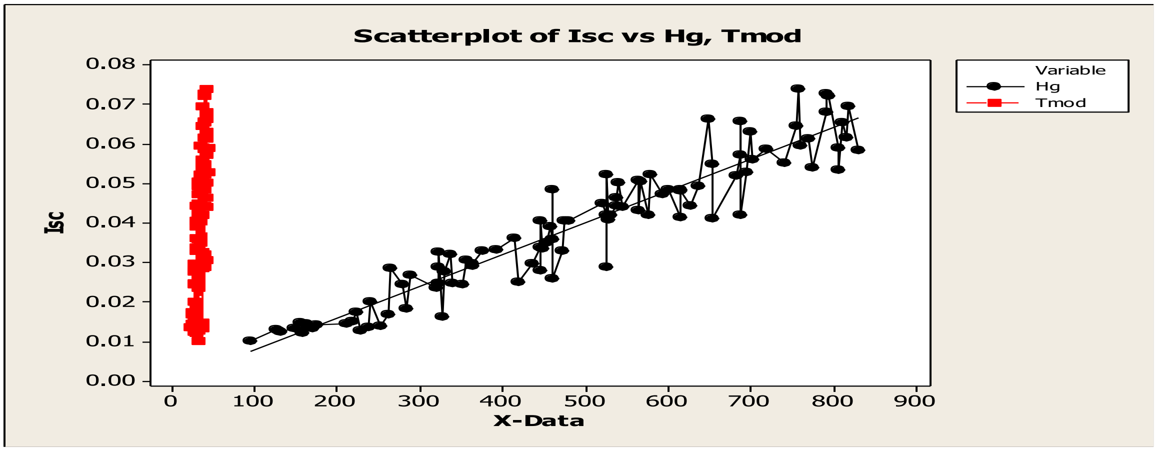

Figure 11: Scatter plot of I_{sc} versus H_g and T_{mod} for the amorphous module

Table 9: Predictor coefficient for the independent variables and the T-test value for equation 7

Predictor	Coefficient	SE Coefficient	T-test	P-value	VIF
Constant	-0.31579	0.07347	-4.30	0.000	
H_g	0.00057380	0.00006293	9.12	0.000	1.6
T_{mod}	0.005149	0.002526	2.04	0.000	1.6

Table 10: Regression Analysis of variance (ANOVA) of the model for equation 7

Source	Degree of freedom	Sum of Squares	Mean Square	F-test	P-value
Regression	2	1.84837	0.92418	90.06	0.000
Residual Error	97	0.99535	0.01026		
Total	99	2.84372			

S = 0.106068 R-Sq = 65.0%   R-Sq(adj) = 64.3%

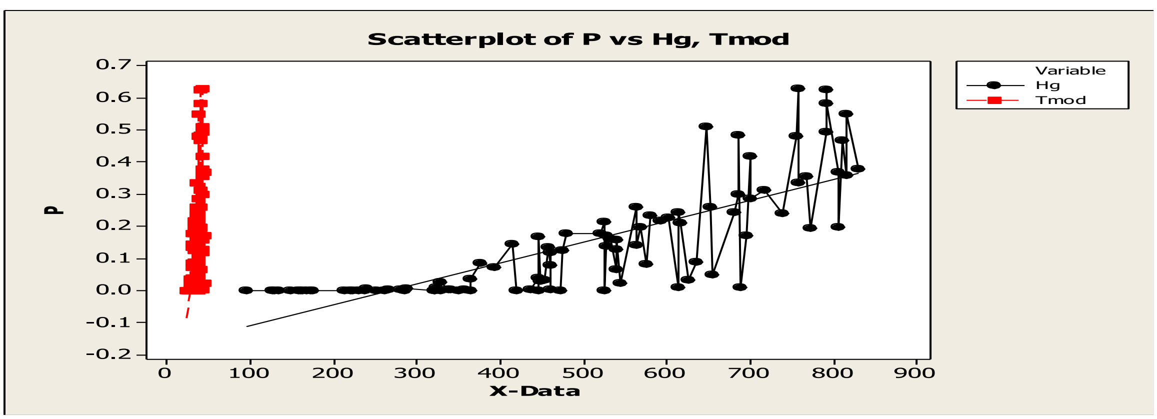

Figure 12: Scatter plot of P versus H_g and T_{mod} for the amorphous module

The regression equation is for P_{max} is $Pmax = -0.324 + 0.000567\,Hg + 0.00542\,Tmod$ 8

Table 11: Predictor coefficient for the independent variables and the T-test value for equation 8

Predictor	Coefficient	SE Coefficient	T-test	P-value	VIF
Constant	-0.32357	0.07330	-4.41	0.000	
H_g	0.00056746	0.0006279	9.04	0.000	1.6
T_{mod}	0.005422	0.002520	2.15	0.034	1.6

Table 12: Regression Analysis of variance (ANOVA) of the model for equation 8

Source	Degree of freedom	Sum of Squares	Mean Square	F-test	P-value
Regression	2	1.84139	0.92070	90.14	0.000
Residual Error	97	0.99072	0.01021		
Total	99	2.83211			

S = 0.101063R-Sq = 65.0% R-Sq (adj) = 64.3%

From Table 12, since the P-value = 0.000 is less than 5% (0.05) level of significance; it can be concluded that there is statistically significant difference in the contributions of the variables H_g and T_{mod} in the model.

This is further explained by the coefficient of determination R^2 = 65.0 % that is 65.0 % of the variable was explained by the model, while only 35 % was unexplained. The model in equation 8 is a good model. Overall lack of fit test is significant at P = 0.000.

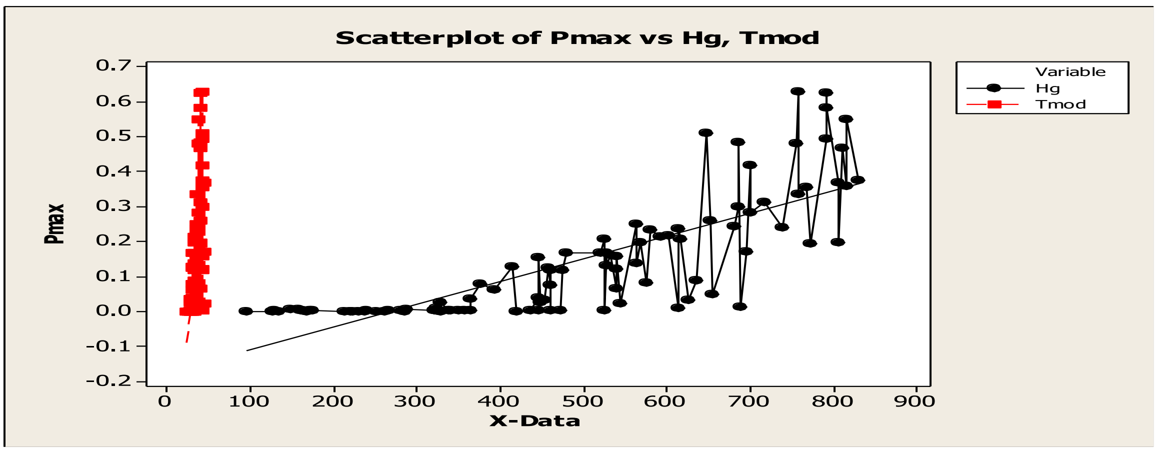

Figure 13: Scatter plot of P_{max} versus H_g and T_{mod} for the amorphous module

Table 13: Correlation Matrix for the Amorphous Module: T_{mod}, H_g, T_a, RH, and WS

	T_{mod}	H_g	T_a	RH
Hg	0.622			
	0.000			
T_a	0.215	0.077		
	0.032	0.444		
RH	-0.581	-0.290	0.080	
	0.000	0.003	0.430	
WS	-0.101	0.419	-0.059	-0.353
	0.319	0.000	0.557	0.000

Cell Contents: Pearson correlation
P-Value

From Table 13, the correlation between T_{mod} and H_g is 0.62 which is high, this show a positive linear relationship between the variables T_{mod} and H_g, furthermore there is significant relationship between the variables at 5% level of significant with P-value = 0.000. There is an average negative correlation between RH and T_{mod} of -0.58 and there is significant relationship between the variables at 5 % level of significance with P-value = 0.000. However, there is low correlation among RH and H_g of -0.29, RH and T_a of 0.08, T_a and T_{mod} of 0.22, T_a and H_g of 0.08, WS and T_{mod} of -0.10, WS and H_g of 0.42, WS and T_a of -0.06, WS and RH of -0.35.

3.2 Comparison between Measured and Predicted Performance Variables

The predicted performance variables at different levels of irradiance and module temperature were plotted with the measured variables for amorphous silicon module and presented in Figures 14 – 17. Here it is seen that the predicted short-circuit current shows almost exact profile with the measured short-circuit current. This again confirms that output current of the PV module has linear relationship with solar irradiance and module temperature while output voltage and power have non-linear relationship with these ambient parameters.

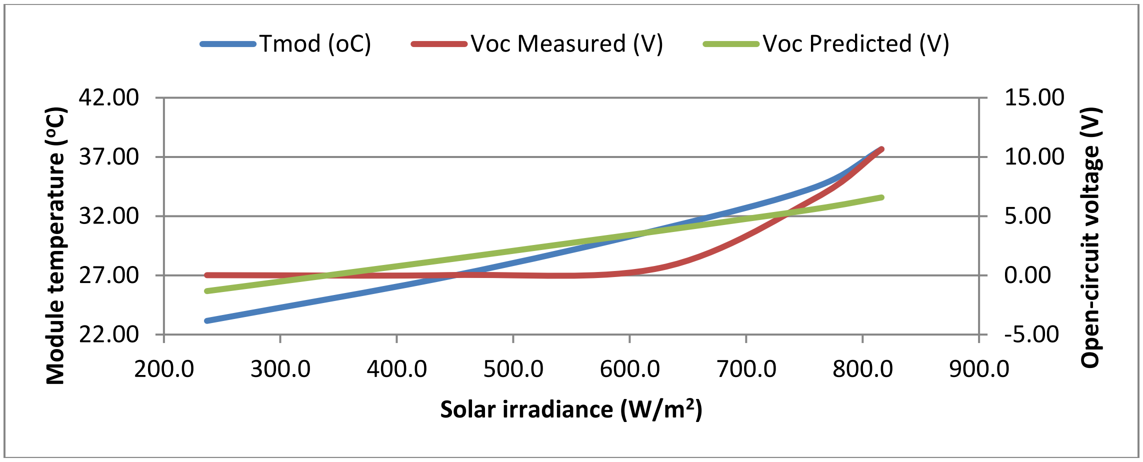

Figure 14: Measured and predicted open-circuit voltage with module temperature as a function of solar irradiance

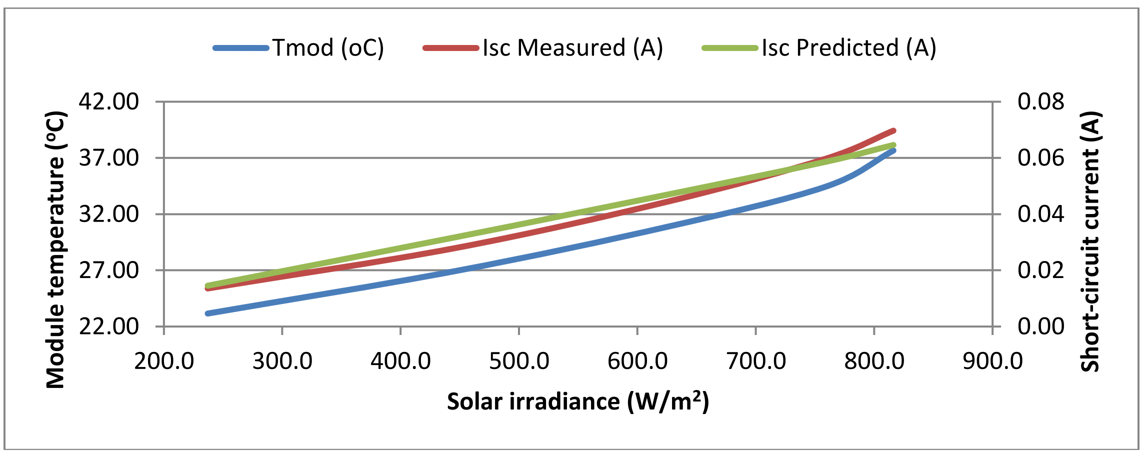

Figure 15: Measured and predicted short-circuit current with module temperature as a function of solar irradiance

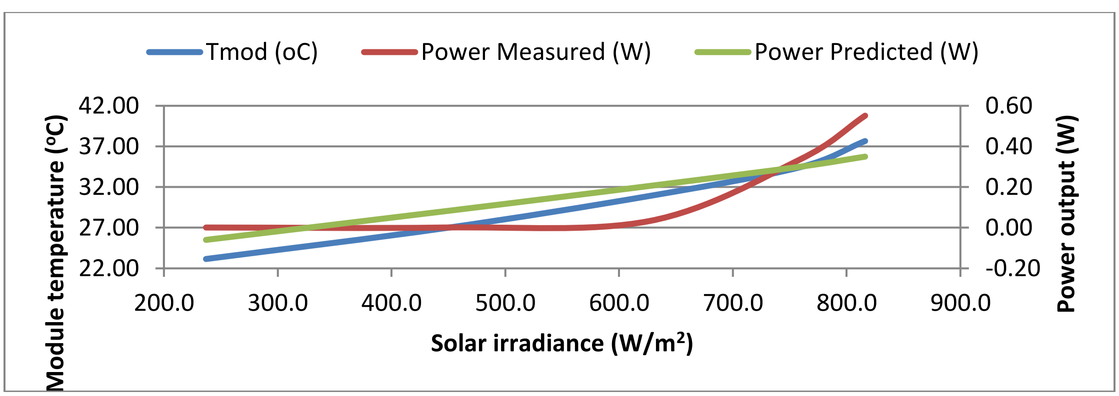

Figure 16: Measured and predicted power output with module temperature as a function of solar irradiance

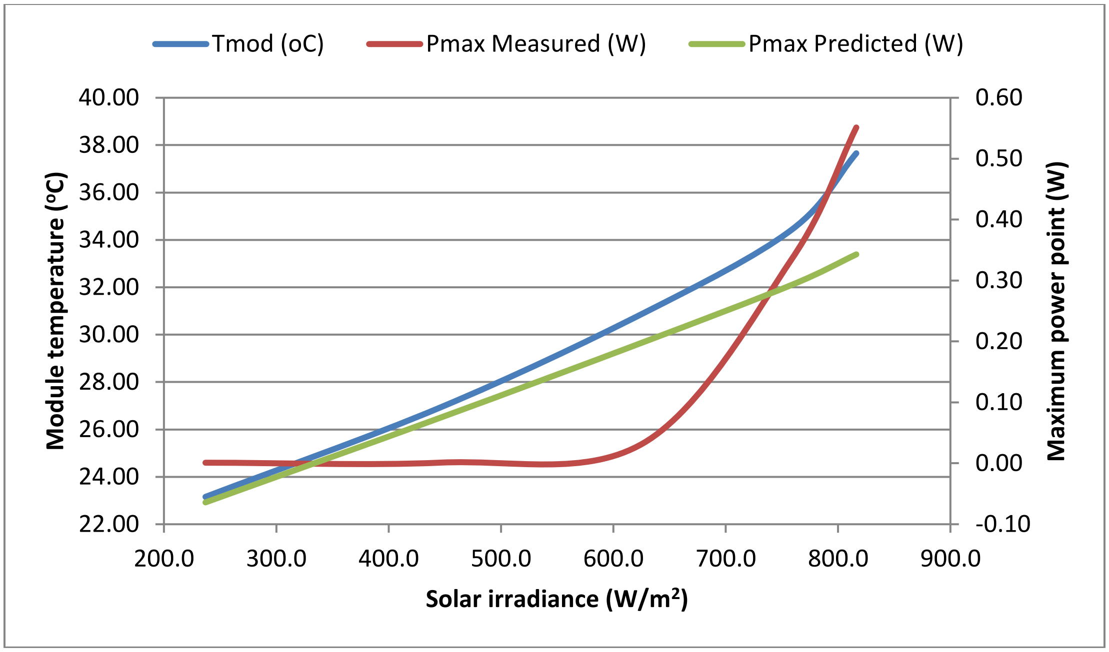

Figure 17: Measured and predicted maximum power with module temperature as a function of solar irradiance

4.0 CONCLUSION

The outdoor characterisation and performance evaluation of the amorphous photovoltaic module in Minna local environment reveals that actual values of performance variables of the module differ greatly from the manufacturer's specifications. The magnitude of the difference between STC specification and the realistic outdoor performance, in this particular study, points to the fact that over specified modules are entering our local market. The maximum power output achieved for the module at irradiance of 1000 W/m^2 was 0.652 W representing 6.52 % of the manufacturer's power specification. While maximum efficiency peaked at irradiance of 536.5 W/m^2 with efficiency value of 3.61 %. This maximum value then dropped steadily with increase in irradiance and, at 1000 W/m^2, reduced to 2.25 % as against manufacturer's specifications of 33 %. Similarly, it was observed that the module did not record 25^{o}C module temperature at irradiance of 1000 W/m^2 as used in STC specifications by the manufacturer. Module temperature was therefore observed to have significant influence on the general performance of the module. In addition to the temperature effects on the performance of the module, some non-intrinsic effects like module mismatch, dust and ohmic losses can contribute to some fraction of the observed reduction in output performances (Causi *et al.*, 1995; Ugwuoke and Okeke, 2012).

The prediction models at different levels of irradiance and module temperature for the performance variables resulting from this work are all good, judging by statistical index, and are as follows: $Voc = -6.46 + 0.0109\,Hg + 0.110\,Tmod$

$Isc = -0.0159 + 0.000072\,Hg + 0.000577\,Tmod$

$P = -0.316 + 0.000578\,Hg + 0.00515\,Tmod$

$Pmax = -0.324 + 0.000567\,Hg + 0.00542\,Tmod$

REFERENCES

Almonacid, F., Rus, C., Hontoria, L., Fuentes, M. and Nofuentes, G. (2009). Characterisation of Single-Crystalline Modules by Artificial Neural Networks, J. Renew. Ener., 34 (4): 941-949.

Bajpai, S.C. and Gupta, R.C. (1986). Effects of Temperature Changes on the Performance of Single-crystalline Solar Cells. Nig. J. of Sol. Ener., 5: 35-41.

California Energy Commission: Energy Development Division. (2001). A Guide to PV System Design and Installation, California, USA.

Causi Li, S., Messana, C., Noviella, G., Paretta, A. and Sarno, A. (1995). Performance Analysis of Single Crystal Silicon Modules in Real Operating Conditions. In Proc. 13th European Photovoltaic Solar Energy Conference (EUPVSEC), Nice, France, pp 11-14.

Midwest Renewable Energy Association Fact Sheet: Off Grid PV Systems (2013). Accessed from www.doe.erec@nciinc.com on 13th May, 2013.

Okafor, E.N.C. and Joe-Uzuegbu, C.K.A. (2010). Challenges to Development of Renewable Energy for Electric Power Sector in Nigeria. Inter. J. of Academic Research, 2 (2), 211-216.

Strong, S.J. and Scheller, W.G. (1991). "The Photovoltiac Room". 2nd ed. Sustainability Press, Chap. 2, Massachusetts, pp 5-7.

Ugwuoke, P.E. and Okeke, C.E. (2012). Performance Assessment of Three Different PV Modules as a Response of Solar Insolation in South Eastern Nigeria, Inter. J. of Applied Sc. and Tech., 2 (3), 319-327.

Ugwuoke, P.E. (2005). Characterisation and Performance Evaluation of Crystalline and Amorphous Photovoltaic Modules in Nsukka Under Field Conditions. PhD Thesis, Department of Physics and Astronomy, University of Nigeria, Nsukka, 3-39.

Ugwuoke, P.E., Ezema F.I. and Okeke C.E. (2005). Performance Response of Single-crystalline PV Modules to Some Atmospheric Parameters at Nsukka, Nig. J. of Space Research. 3 (2), 183-190.

Umar I.H. (1999). Research and Development and Energy Crisis in Nigeria. In Proc. of 1999 Technology Summit, Abuja, Nigeria, pp 39-42.